27/28th International Conference
ENGINEERING MECHANICS 2022
Milovy, Czech Republic, May 9 –12, 2022
Paper **#17,** pp. 217–220, doi: 10.21495/51-2-217

COMPARISON OF THE RESULTS OF ANALYTICAL AND FEM STRESS CALCULATIONS OF THE SPHERICAL NANOINDENTATION

Kovář J.*, Fuis V.**

Abstract: *This paper focuses on the comparison of the calculation of stress fields under the spherical indenter determined with analytical and FEM calculations and the identification of the most common cracks initiation reasons. The most used theory for the description of the contact of sphere and half-space was derived by Hertz. Huber extended this theory to calculate the stress field under the indenter. If every component of stress tensor is known, the principal stresses can be derived. The analytically calculated stresses were verified with the FEM and the initiation and growth of the most common cracks (ring, conical) at spherical indentation was explained.*

Keywords: Hertz theory, Spherical indentation, Fused silica, Nanoindentation, Conical crack.

1. Introduction

The calculation of the contact pressure at the contact of sphere and half-space is based on the Hertz theory (Hertz, 1881). It was derived with the assumptions of isotropic linear-elastic material of the specimen and indenter, the small curvature of the indenter ($a/R < 0.1$, where a is the contact radius and R is the radius of the indenter) and the smooth contact area (no friction). To simplify the results Hertz introduces the reduced modulus (E_{red})(1) and reduced radius of curvature (R_{red})(2). The inscript i is used for indenter and s for specimen. With these assumptions Hertz created well-known theory, which can be used for the calculation of the indentation curve (3) and maximal contact pressure (4).

$$\frac{1}{E_{red}} = \frac{1-\nu_s^2}{E_s} + \frac{1-\nu_i^2}{E_i} \tag{1}$$

$$\frac{1}{R_{red}} = \frac{1}{R_s} + \frac{1}{R_i} \tag{2}$$

$$F = \frac{4}{3} \cdot E_{red} \cdot h^{\frac{3}{2}} \cdot R^{\frac{1}{2}} \tag{3}$$

$$p_{max} = \frac{3 \cdot F}{2 \cdot \pi \cdot a^2} \tag{4}$$

The assumption of small curvature is related to the expected parabolical contact stress field. This leads to the same equations as can be derived for the indenter with the shape of paraboloid (Huber, 1904). The results without this assumption can be derived by MDR method (Popov, 2019) but leads to the very difficult non-linear equations.

The Hertz theory can be used to determine the stresses on the axis of indentation and in the contact area. To get stress fields for every component of the stress tensor at whole specimen, the Theory by Huber (1904) was derived. It was derived to get stress fields under the paraboloid indenter at indentation of the linear elastic half-space. The paraboloid indenter is the same assumption as uses the Hertz theory, so these equations should work for spherical indenter too, if the assumptions of Hertz theory are valid. Huber derived his equations for calculation of all non-zero components of stress tensor (6 - 9) in cylindrical coordinates with the z as direction of indentation. The variable u (5) was introduced to simplify the equations. These

* Ing. Jaroslav Kovář: Institute of Solid Mechanics, Mechatronics and Biomechanics, Brno University of Technology, Technická 2896/2; 616 69, Brno; CZ, Jaroslav.Kovar@vut.cz

** Assoc. prof. Ing. Vladimír Fuis, Ph.D.: Centre of Mechatronics – Institute of Thermomechanics of the Czech Academy of Sciences – branch Brno and Faculty of Mechanical Engineering, Brno University of Technology, Technická 2896/2; 619 69, Brno, CZ, fuis@it.cas.cz

equations were derived from the theoretical models, to verify them, the results will be compared with the FEM results and then the principal stresses will be calculated.

$$u\,(r,z) = \frac{1}{2}\cdot\left[r^2+z^2-a^2+\sqrt{(r^2+z^2-a^2)^2+4a^2\cdot z^2}\right] \tag{5}$$

$$\sigma_r(r,z) = p_{max}\cdot\left\{\frac{(1-2\mu)\cdot a^2\cdot\left[1-\left(\frac{z}{\sqrt{u}}\right)^3\right]}{3\cdot r^2}+\frac{a^2\cdot u\cdot\left(\frac{z}{\sqrt{u}}\right)^3}{u^2+a^2\cdot z^2}+\frac{z}{\sqrt{u}}\cdot\left[\frac{(1-\mu)\cdot u}{a^2+u}+\frac{(1+\mu)\cdot\sqrt{u}\cdot\arctan\frac{a}{\sqrt{u}}}{a}\cdot-2\right]\right\} \tag{6}$$

$$\sigma_t(r,z) = -p_{max}\cdot\left\{\frac{(1-2\mu)\cdot a^2\cdot\left[1-\left(\frac{z}{\sqrt{u}}\right)^3\right]}{3r^2}+\frac{z}{\sqrt{u}}\cdot\left[2\mu+\frac{(1-\mu)\cdot u}{a^2+u}-\frac{(1+\mu)\cdot\sqrt{u}\cdot\arctan\frac{a}{\sqrt{u}}}{a}\right]\right\} \tag{7}$$

$$\sigma_z(r,z) = -p_{max}\cdot\left(\frac{z}{\sqrt{u}}\right)^3\cdot\frac{a^2\cdot u}{u^2+a^2\cdot z^2} \tag{8}$$

$$\tau_{rz}(r,z) = -p_{max}\cdot\frac{r\cdot z^2}{u^2+a^2\cdot z^2}\cdot\frac{a^2\cdot\sqrt{u}}{a^2+u} \tag{9}$$

2. Methods

The analytical and FEM calculations of the spherical indentation were done. The model of geometry is in the Fig 1. Spherical indenter had a radius $R_i = 10$ µm and it was made from diamond with $E_i = 1\,141\,000$ MPa and $\nu_i = 0.07$ (Kovář, 2019). The half-space was from fused silica modelled as bilinear model of material with elastic parameters $E_s = 72\,000$ MPa and $\nu_s = 0.17$ (Kovář, 2019). To compare the stress fields, the displacement of the indenter was chosen as 0.2 µm, to make no plastic deformation. To asses when the elastic theory can be used the FEM calculation was done with displacement 2 µm and the bilinear model of plasticity with the yield stress $\sigma_y = 4600$ MPa and isotropic hardening $n = 10\,000$ MPa was used.

The 2D axisymmetric model with boundary conditions as in Fig. 1 was used for FEM. The indenter was loaded by the displacement of its upper edge and the reaction force was calculated at the lower edge of the specimen. The mesh was created from PLANE 183 elements, refined in the contact region (Fig. 2). The calculation was divided into more than 100 substeps, to achieve accurate results with fast convergence.

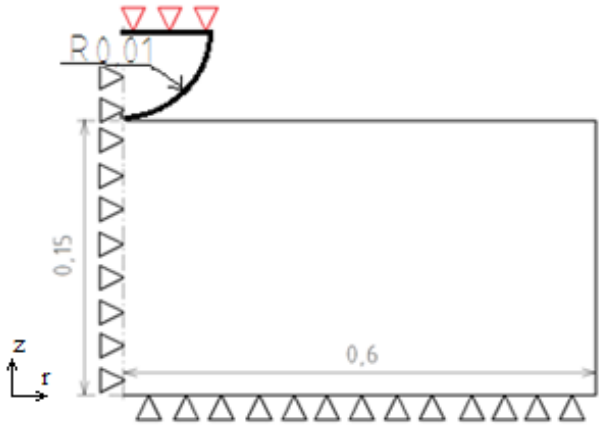

Fig. 1: Model of spherical indentation

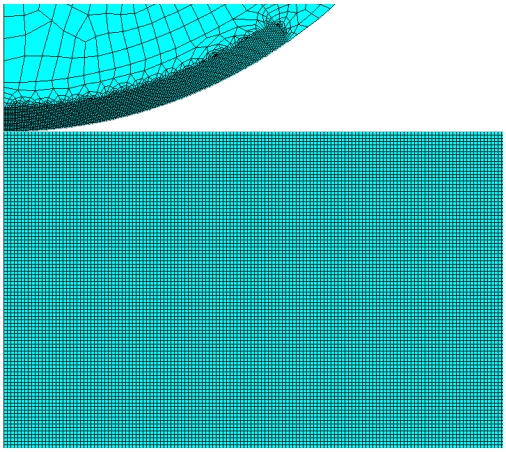

Fig. 2: Mesh used for FEM- detail

The analytical calculations of the stresses were calculated and plotted in Matlab. As every stress component was known in each point of graph, the principal stresses were calculated with equation (10) (Janíček, 2004), where I are invariants of stress tensor. The cubic equation was for each point solved in Matlab too and then the graphs of principal stresses were plotted.

$$\sigma^3 - I_1\cdot\sigma^2 + I_2\cdot\sigma - I_3 = 0 \tag{10}$$

3. Results and discussion

The indentation curves from FEM and analytical calculations were compared (Fig. 3). These two curves are nearly the same until the indentation force 100 mN and then they start to diverge. It is caused by the

plastic deformation, which is neglected in analytical calculations, because the first plastic deformations in the specimen already occurred at indentation force 32 mN. Then the stress fields were plotted at the displacement of the indenter 0.2 μm and indentation force 26.5 mN, where the analytical calculations should be valid. These stresses were plotted from analytical calculation and FEM and compared (Fig.4). The results show nearly the same values, which verifies the analytical calculations. The analytical calculation has a singularity at the contact surface and axis of symmetry. In these points, the infinite values were obtained (Huber, 1904). To eliminate this problem, the results near these points were plotted where the analytical calculation still gives correct values.

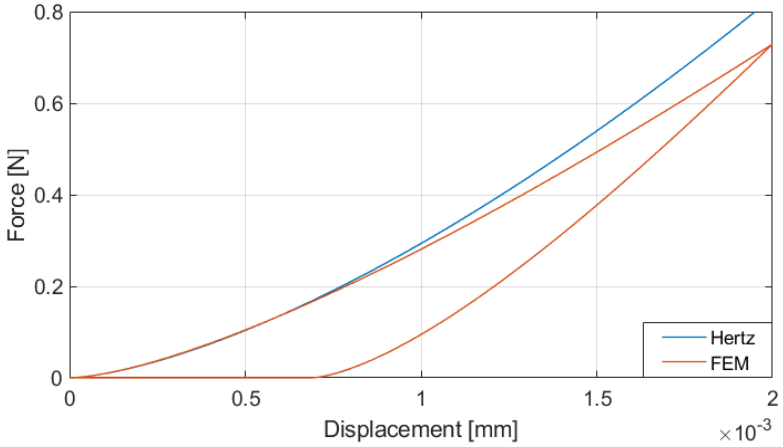

Fig. 3: Indentation curves

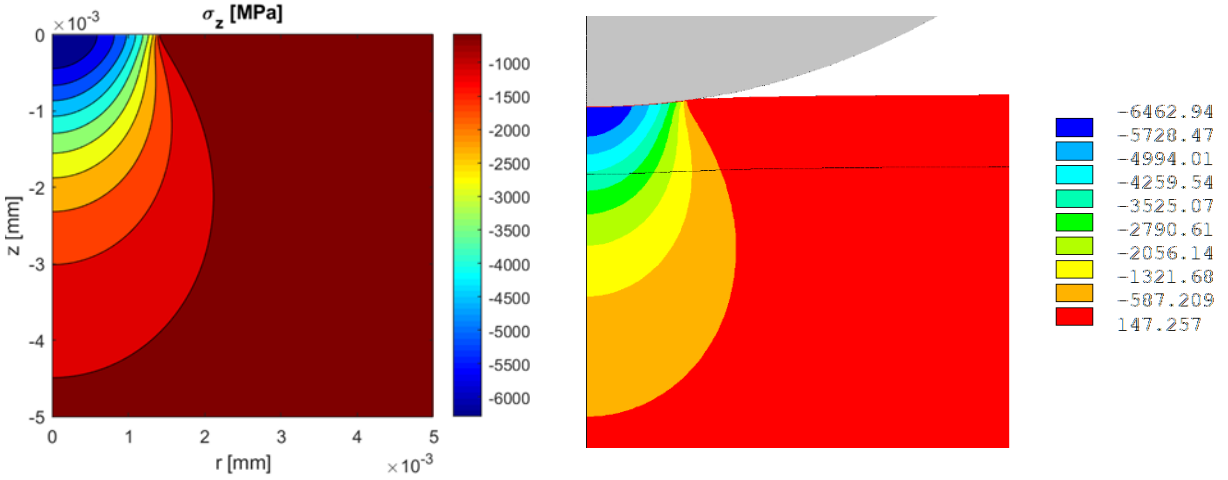

Fig. 4: Z component of stress [MPa] *(analytical calculation – left, FEM - right)*

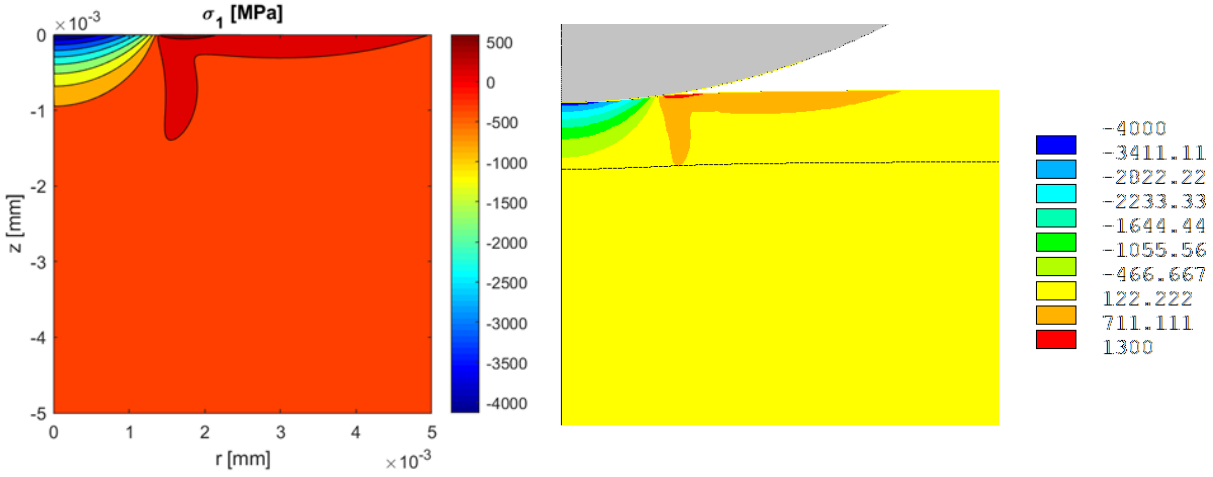

Fig. 5: First principal stress [MPa] *(analytical calculation – left, FEM - right)*

The same values of the first principal stress as in the FEM calculation were determined by calculation with eq. (10) (Fig. 5). The positive values of the first principal stress are critical for the formation and the growth of cracks. At the spherical nanoindentation of fused silica, the ring cracks and conical cracks can form (Tillet, 1956) (Fig. 6). The crack often grows perpendicular to the direction of the first principal stress. These directions were calculated by analytical equations from (Janíček, 2004) (Fig. 6). Only the vectors of the positive values of the first principal stresses are shown in this figure. The ring cracks are often created at the surface before the contact area. It is caused by the maximum of the first principal stress. The conical cracks are initiated at the end of contact area and then grow perpendicular to the first principal stress. As the Fig. 6 shows, this direction is heading into the body and forms the crack with conical shape.

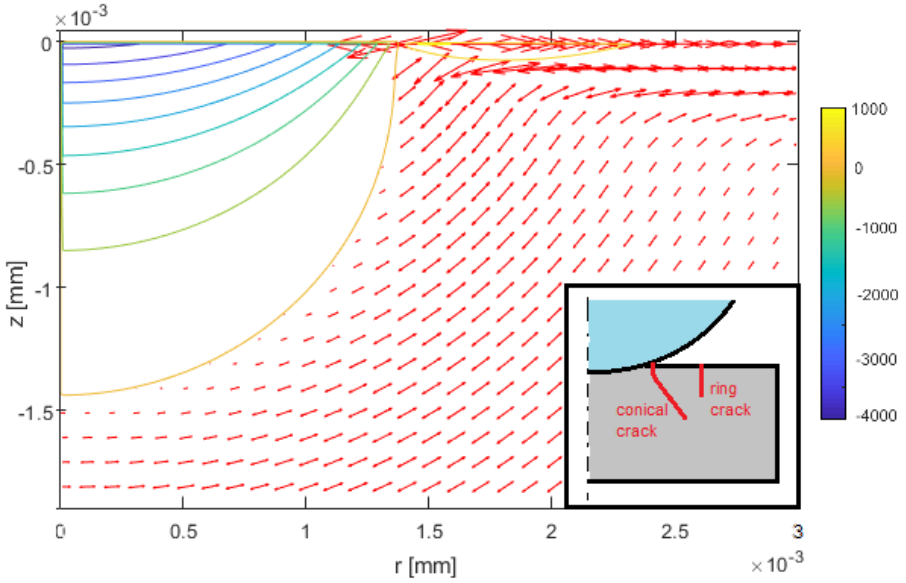

Fig. 6: Directions of the positive first principal stresses and their values [MPa]

4. Conclusion

The indentation curves calculated by the Hertz theory and FEM method for spherical indentation of fused silica were compared. The Hertz theory gives the accurate results, if the assumptions of analytical calculations are met. When the plasticity occurs the indentation curve from FEM gives still more lower values. The stress fields were calculated by the theory derived by Huber (1904). This theory gave the similar results of stresses as commonly used FEM.

With the use of analytical calculations, the principal stresses were calculated and the direction of the first principal stress was determined. The cause of the initiation of the ring and conical cracks was determined. The ring cracks initiate in the point of maximal first principal stress and the conical cracks initiate at the border of contact area and grow perpendicularly to the first principal stress. Although the Hertz theory is limited to elastic deformation, these two types of cracks are commonly observed at the spherical fused silica nanoindentation. The future work will be aimed at the assessment of the probability of the crack initiation.

Acknowledgement

This study was realized with the support by the grant FSI-S-20-6164 and with the institutional support RVO: 61388998.

References

Hertz, H. (1881) Über die Berührung fester elastischer Körper. *Journal für die reine und angewandte Mathematik*. 92, 156-171.

Huber, M. T. (1904). Zur Theorie der Berührung fester elastischer Körper. *Annalen der Physik*, 319(6).

Janíček, P., Ondráček, E., Vrbka, J. and Burša, J. (2004). *Mechanika těles: pružnost a pevnost I*. CERM. (in Czech)

Kovář, J. and Fuis, V. (2019). FEM simulation of the nanoindentation test with rigid and non-rigid indenter. In Zolotarev, I and Radolf, V., *Engineering mechanics 2019*, Inst. of Thermomechanics, CAS, Prague, pp. 189-192.

Popov, V. L., Heß, M. and Willert, E. (2019). Handbook of Contact Mechanics: Exact Solutions of Axisymmetric Contact Problems. Springer, Berlin, Heidelberg.

Tillett, J. P. A. (1956). Fracture of Glass by Spherical Indenters. *Proceedings of the Physical Society. Section B*, 69(1).